EUROPHYSICS LETTERS 1 June 2006

Europhys. Lett., **74** (5), pp. 847–853 (2006)
DOI: 10.1209/epl/i2006-10037-5

Variable profiles of plasma pulses generated from high-k dielectric barrier discharge

E. H. Bentefour[1], H. M. J. Bastiaens[2] and R. M. Hofstra[1]

[1] *Nederlands Centrum voor Laser Research (NCLR) B.V.*
P.O. Box 2662, 7500 CR, Enschede, The Netherlands
[2] *Group of laser physics and non-linear optics, Faculty of Science & Technology*
University of Twente - Enschede, The Netherlands

received 12 January 2006; accepted in final form 6 April 2006
published online 3 May 2006

PACS. 52.50.Dg – Plasma sources.
PACS. 52.80.Tn – Other gas discharges.

Abstract. – With a specific design of a high-k dielectric barrier discharge, we observed plasma pulses with variable spatial profiles as a consequence of excitation by a high-voltage pulse at different pressures. The dependence of the profile of the generated plasma pulses on the charging voltage and the operating gas (air) pressure is described and the description of their temporal and spatial build-up mechanism is given. We demonstrate that the profile variation of the plasma pulses is caused by the co-existence of dipole switching-based electron emission and field electron emission from triple junctions. Finally, we propose a scheme describing the interaction of these two electron emission mechanisms that leads to the pressure dependence of plasma pulse profile.

Introduction. – Dielectric barrier discharge (DBD) is an established technique for generating cold plasmas. It has found several applications such as in lighting, ozone production, surface modification, localized material growth or spectroscopic studies. Another important application of DBD is the building of electron beam sources with very high current densities of up to $100\,\mathrm{A/cm^2}$ [1–5]. The electron emission mechanisms that take place in these devices were subject to several studies [6–10]. It was ascribed initially to a fast spontaneous polarization switching or fast field-induced phase transition [11, 12]. Plasma-assisted electron emission was also demonstrated [13–15]. Moreover, a plasma may be initiated at any dielectric surface by field emission at the triple point junction (ceramic-metal-gas) [16]. Despite about fifteen years of research that deals with this issue, there is no definite and unique view about the physics of the phenomenon. Generally, most researchers attribute the origin of electron emission to either field emission at triple point junctions or to polarization switching, both forward polarization reversal and back-switching of the ferroelectric domains [6, 17].

In this paper, we report a novel aspect of the operation of high-k ceramic cathode-based electron beam device, which offers the option to tune the full width half-maximum (FWHM) of the profiles of the generated plasma pulses. In the first section of this paper, we report the observation of the spatial dependence of plasma pulse profiles generated as consequence of excitation by a high voltage pulse at different pressures or, alternatively, at different voltage amplitudes for a fixed pressure. In the second section, we establish the link between the generated electron beam density and the consequent plasma pulse profile. In the third section,

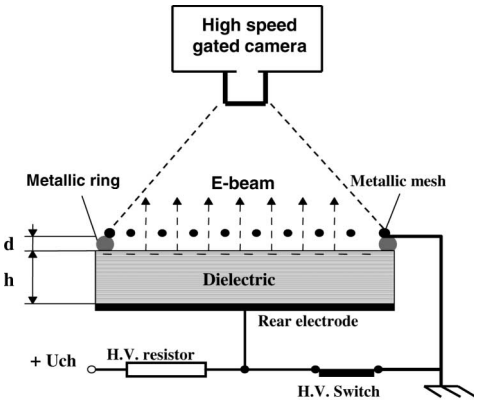

Fig. 1

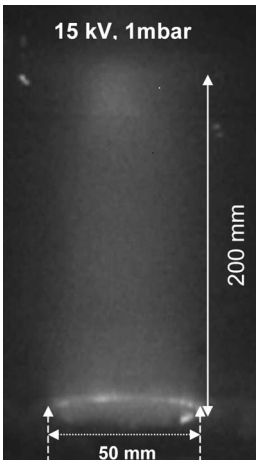

Fig. 2

Fig. 1 – Experimental setup showing both the electron beam generator and the driving electrical circuit.

Fig. 2 – A side view of the electron beam generated at 15 kV and 1 mbar at repetition rate of 90 Hz.

we demonstrate how the observed phenomenon can be explained by the co-existence of polarization reversal and/or domain switching-based electron emission and field electron emission from triple junctions as two different electron emission mechanisms.

Experimental set-up. – Figure 1 illustrates the experimental arrangement of our electron beam device. It consists of a dielectric barrier discharge module as the electron beam generator unit. This module is made of a $BaTiO_3$ ceramic cylinder of 5 cm diameter and 7 mm thickness. The static relative dielectric permittivity of the ceramic, calculated from the capacity at room temperature, is about $\varepsilon_r = 2300$. A metallic ring, made of stainless-steel wire, delimits the dielectric surface. It also serves as a spacer to hold a stainless-steel metallic mesh having geometrical transparency of 65%. The distance d between the front surface of the dielectric ($BaTiO_3$) and the output metallic mesh was fixed to about 2 mm. A DC high voltage is applied to the metallic rear electrode of the dielectric sample. Then the rear electrode is short-circuited to earth by means of a thyratron switch inducing a fast electric-field reversal between the dielectric rear electrode and the grounded metallic mesh anode. Consequently, a discharge current and an electron beam current flow in the circuit of the device. Those two currents are monitored using Rogowski coils, the discharge voltage is measured with a Tektronix high-voltage probe.

To study the generation mechanism of the electron beam from our device, we monitored the light emission (fluorescence) caused by the generated electron beam using a fast-gated ICCD camera with a gating time of 1 ns. This technique allows us to trace the plasma pulse formation with very high temporal resolution. We also monitored the current density of the generated electron beam *vs.* the pressure and the charging voltage. The measurement of the electron beam current density was made with a collimated Faraday cup placed at 15 mm from the ceramic cathode surface.

Results and discussion. – The generation of an electron beam from our device is visually evident as seen in fig. 2. This picture shows a side view of the plasma pulse (fluorescence) generated at 15 kV and 1 mbar at a repetition rate of 90 Hz. The pulse duration of the

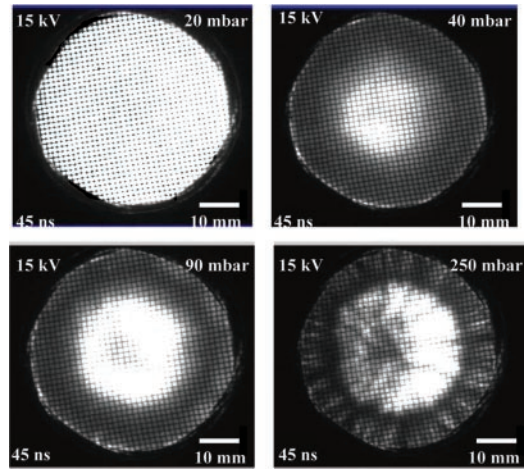

Fig. 3 – Series of snapshots of plasma pulses generated at 15 kV and for different pressures. The pictures are taken at about the same time with respect to the beginning of the high-voltage excitation pulse.

generated electron beam, measured with collimated Faraday cup, is about 150 ns, with rise time equal to 45 ns. The maximum current density that we could generate reaches $7\,\mathrm{A/cm^2}$. Our result is comparable to the result reported in ref. [12], but for unknown reasons it is about ten times smaller than what is reported in ref. [5].

The fast ICCD imaging, viewing from above, reveals that, depending on the experimental conditions (charging voltage and operating gas pressure), the plasma pulse varies in size. Below a certain pressure threshold, the plasma pulse covers all the emitting area of the ceramic. Above this pressure threshold the plasma pulse becomes confined in the center of the dielectric cathode surface; then, depending on the applied charging voltage and gas pressure, the size of the plasma pulse reduces or becomes larger. Figure 3 shows a series of snapshots of the plasma pulses. This experiment was done at the charging voltage of 15 kV and at various gas pressures. All the pictures are taken about 45 ± 2 ns after the high-voltage excitation pulse. This timing corresponds to the average rise time of the device. Other series of measurements have been taken at lower charging voltages, respectively at 5 kV and 10 kV. In all these series of pictures the FWHM of the profile of plasma pulses stays equal to the device radius up to certain pressure threshold then suddenly drops to a minimum value and starts to increase again with increasing pressure. The distribution of the plasma pulse is more or less circular and its center coincided, to a good approximation, with the center of the dielectric barrier surface. Figure 4 summarizes the evolution of the FWHM of the plasma pulse profile *vs.* the operating gas pressure for three charging voltages (5 kV, 10 kV and 15 kV). The values reported in this figure are the average of the FWHM measured over different directions of the profile of the photographed fluorescence spot. The upper limit of the pressure range was imposed by the discharge quality in terms of stability and spatial uniformity. At lower applied voltage of 5 kV, increasing the pressure further than 150 mbar causes an incomplete discharge and thus a deterioration of the plasma pulse shape. For the case of 15 kV, a further increase of the pressure (over 300 mbar) causes the discharge to become more filamentary and also deteriorates the plasma pulse shape. The last picture in the series of photographs shown in fig. 3 shows the beginning of this filamentary discharge behavior. The transitional behavior of the profile of plasma pulses shown in fig. 3 (occurring, respectively, around 25 mbar in the

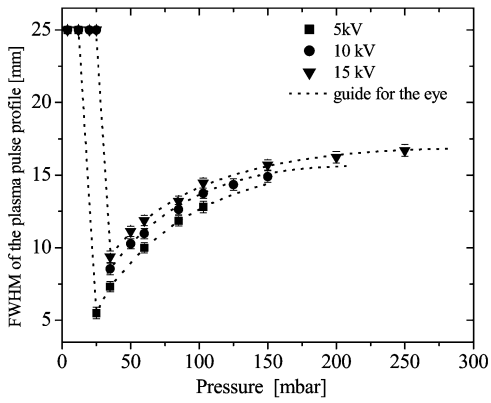

Fig. 4

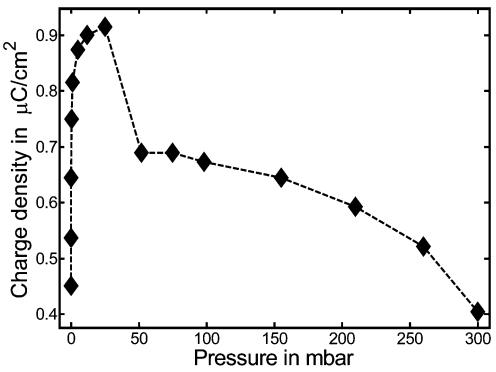

Fig. 5

Fig. 4 – Evolution of the generated plasma pulse profile *vs.* the pressure for three charging voltages. Note that the FWHM of plasma pulse profile can be tuned continuously to vary by at least 3 times of the starting value.

Fig. 5 – Behavior of the total charge density of the electron beam *vs.* the pressure.

case of 5 kV and around 35 mbar in the cases of 10 kV and 15 kV) is an important finding. From our knowledge, it is the first time that such behaviour is investigated. As the imaged fluorescence is the signature of accelerated electrons, we believe it can be assumed that the observed transition in the plasma pulse profile expresses similar behavior in the corresponding electron beam. This assumption can be verified, in principle, by the analysis of the evolution of the total emitted charge *vs.* the pressure for a fixed high-voltage excitation pulse. We evaluate the total charge of the electron beam by integrating the area under the current pulse measured with the collimated Faraday cup. Figure 5 shows the result of this operation by plotting the total electron beam charge Q against the pressure for a pulse excitation voltage of 15 kV. The result confirms the earlier assumption and, in fact, shows sudden drops, in a form of transitional behavior, of the total charge. This transition takes place around 35 mbar, thus in good correspondence with the transition observed in the plasma pulse profile at a voltage of 15 kV. At this level, we are convinced that the electron beam formation mechanism, taking place in our device, is pressure and high-voltage amplitude dependent.

More detailed imaging, using the —nanosecond gating time— ICCD camera, of the earlier stage of the plasma pulse generation was used to obtain additional understanding of the electron beam formation mechanism. Images captured at the beginning of the operation cycle of the device in both pressure regions before and after the transitional behavior show, respectively, the presence of two different physical processes. Figure 6 shows the process of the plasma pulse build-up before and after the pressure-induced transition. At a pressure below the transition (20 mbar), the successive pictures of series I of fig. 6, shows that the discharge begins from the metallic ring that surrounds the dielectric cathode surface and flows, very rapidly, to the center of it. The plasma pulse then builds-up uniformly over the whole area inside the metallic ring. At higher pressure, above the transition (50 mbar), the formation of the plasma pulse occurs in a different way. Simultaneous to the appearance of the plasma (fluorescence) at the metallic ring (process 1), plasma appears also at the center of the dielectric surface (process 2) as shown in the first picture of series II of fig. 6. The build-up of the plasma pulse happens in such a way that the plasma in the center of the dielectric grows faster, an apparent transfer of plasma from the plasma at the edge of the metallic ring

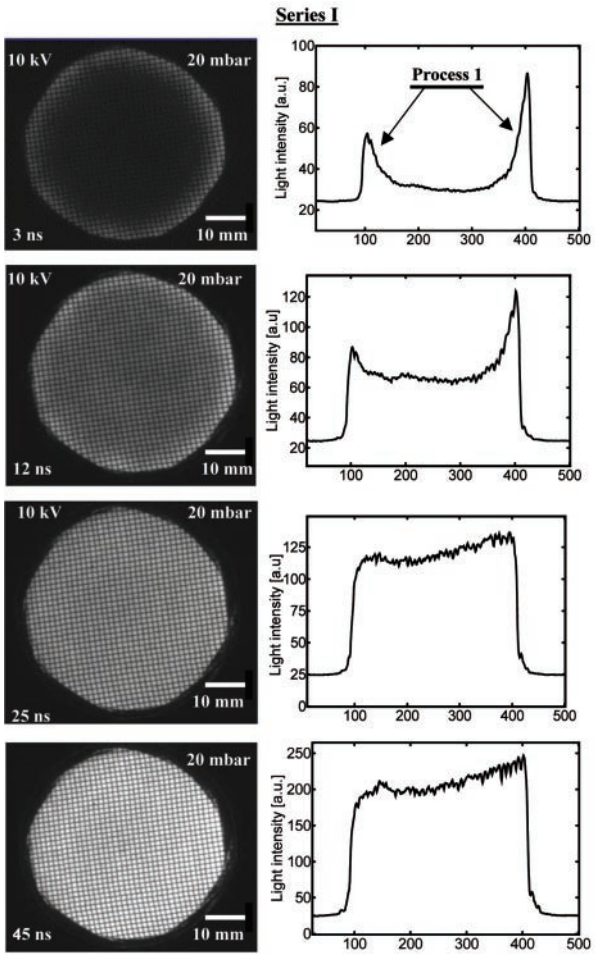

Fig. 6 – Process of plasma pulse build-up at the charging voltage of 10 kV before and after the pressure-induced transition point. The series I corresponds to 20 mbar.

to the plasma in the center of the dielectric seems to be taking place and contributing to the formation of the final plasma pulse. The pictures 3 and 4 of the same series and their corresponding profiles indicate the apparent transfer of plasma (indicated by the arrows) from the metallic ring toward the center of the dielectric. A dynamic viewing (movie) of the electron beam generation in this case (10 kV, 50 mbar) highlights this transfer in more detail.

Upon this analysis, it is reasonable to think that there are two parallel electron emission processes that contribute to the generation of the electron beam. These two processes occur independently of each other. One is electron emission due to field emission caused by the large tangential component of the electric field at the triple point junctions (edge of the metallic ring) and the other is dipole switching electron emission. The first mechanism is potentially present at any pressure and it occurs in the vicinity of the metallic ring that surrounds the ceramic cathode as shown in the first picture of series I in fig. 6. This emission mechanism is followed by a plasma flashover of the dielectric surface. The second mechanism is dipole switching and domain-reversal–based electron emission. This mechanism is also, in principle, present at every pressure. We believe that the transitional behavior observed in the plasma

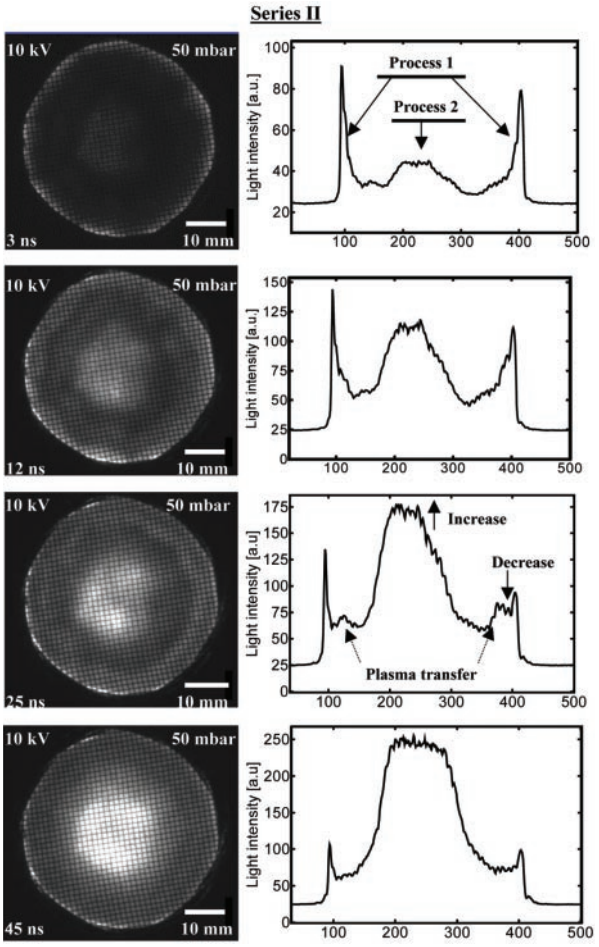

Fig. 6 – (*Continued.*) The same as for series I but at 50 mbar.

pulse profile, respectively in the total charge of the electron beam, is a result of the competition between these two processes. We justify our conclusions as follows.

The competition between the two electron emission mechanisms, mentioned above, is related to the speed with which each process is established with respect to the other: The relaxation time of dipole switching depends on the strength of the applied electric field. It becomes faster with increasing the applied electrical field amplitude [18–20]. It is shown that it could be shorter than 10 ns [21]. The speed of the plasma flashover, that follows the field emission of electrons from the triple junctions, decreases with the pressure [22]. Thus, for fixed high-voltage excitation amplitude, the relaxation time of the dipole switching is constant while the plasma flashover of the dielectric surface slows down with increasing pressure. Thus before the transition point (10 kV/35 mbar), the plasma flashover develops faster than the dipole-switching–based electron emission process and screens it from ICCD detection. Increasing the pressure slows down the plasma flashover and provides enough time for the dipole switching electron emission process to appear. Obviously, it appears first in the center of the ceramic, which is the farthest point from the flashover plasma wavefront. As the gas pressure increases, the plasma flashover becomes slower and the dipole switching electron emission mechanism ap-

pears over a larger area explaining why the plasma pulse profile becomes wider again after the transition. To support our analysis, we carried out a second experiment in the absence of the field electron emission mechanism. To do so, we modified the design of the same electron beam source by removing both the metallic ring and the metallic mesh in order to eliminate the triple point junctions. In this experiment, it was possible to generate an electron beam of about the same maximum current density as reported earlier but neither the measurement of the electron beam current nor the imaging of the plasma pulse showed any transitional behavior.

Conclusions. – In summary, we have shown that our design of dielectric-barrier discharge-based electron source has specific and unique features. It allows the observation of two different electron emission mechanisms and offers the option to study their interactions. These interactions result in a competition-like process that leads to a form of electron beam reduction. The pressure controls this competition and leads to a transitional behavior and, more interestingly, to the variation of the profile of the generated plasma pulses.

* * *

One of the authors, EHB, gratefully acknowledges the financial support of the European commission in the form of Marie-Curie research grant, HPMI-CT-2001-00145.

REFERENCES

[1] Gundel H., Riege H., Handerek J. and Zioutas K., *Appl. Phys. Lett.*, **54** (1989) 2071.
[2] Gundel H., Reige H., Handerek J. and Zioutas K., *Appl. Phys. Lett.*, **69** (1991) 975.
[3] Ivers J., Schachter L., Nation J., Kerslik G. and Advani R., *J. Appl. Phys.*, **73** (1993) 2667.
[4] Riege H., *Nucl. Instrum. Methods Phys. Res. A*, **340** (1994) 80.
[5] Mitko S. V., Udalov Y., Peters P. J. M., Ochkin V. N. and Boller K. J., *Appl. Phys. Lett.*, **83** (2003) 2760.
[6] Rosenman G., Shur D., Krasik Ya. E. and Dunaevsky A., *Appl. Phys. Rev.*, **88** (2000) 6109.
[7] Golubovskii Yu. B., Maiorov V. A., Behnke J. and Behnke J. F., *J. Phys. D*, **35** (2002) 751.
[8] Kogelschatz U., *IEEE Trans. Plasma Sci.*, **30** (2002) 1400.
[9] Tarasenko V. F. and Yakovlenko S. I., *Plasma Devices Operat.*, **13** (2005) 231.
[10] Jiang B., Kirkman G. and Reinhardt N., *Appl. Phys. Lett.*, **66** (1995) 1196.
[11] Cavazos T., Wilbanks W., Fleddermann C. and Shiffler D., *Appl. Phys. Lett.*, **65** (1994) 2612.
[12] Dunaevsky A., Krasik Ya. E., Felsteiner J. and Dorfman S., *J. Appl. Phys.*, **85** (1999) 8464.
[13] Dunaevsky A., Krasik Ya. E., Felsteiner J. and Sternlieb A., *J. Appl. Phys.*, **90** (2001) 3689.
[14] Boscolo I. and Cialdi S., *J. Appl. Phys.*, **91** (2002) 6125.
[15] Shur D., Rosenman G., Krasik Ya. and Advani R., *J. Appl. Phys.*, **31** (1998) 1375.
[16] Punchkarev V. F. and Mesyats G. A., *J. Appl. Phys.*, **78** (1995) 5633.
[17] Shur D. and Rosenman G., *J. Phys. D*, **32** (1999) 29.
[18] Merz A. J., *Phys. Rev.*, **95** (1954) 690.
[19] Fatuzzo E. and Merz W. J., *Phys. Rev.*, **116** (1959) 61.
[20] Jullian C., Li J. F. and Viehland D., *J. Appl. Phys.*, **95** (2004) 5671.
[21] Jullian C., Li J. F. and Viehland D., *Appl. Phys. Lett.*, **83** (2003) 1196.
[22] Neuber A., Butcher M., Hatfield L. and Krompholz H., *J. Appl. Phys.*, **58** (1998) 3084.